# Multiterminal junctions formed by heating ultrathin single-walled carbon nanotubes

F. Y. Meng,[1,2] S. Q. Shi,[1,*] D. S. Xu,[2] and R. Yang[2]
[1]*Department of Mechanical Engineering, Hong Kong Polytechnic University, Hong Kong, China*
[2]*Institute of Metal Research, Chinese Academy of Sciences, 72 Wenhua Road, Shenyang 110016, China*
(Received 16 June 2004; published 20 September 2004)

Ultra-thin single-walled carbon nanotubes can be welded by heating to form molecular multi-terminal junctions at elevated temperatures without initially introducing structural defects such as vacancies and interstitials. This was demonstrated by classical molecular dynamics simulations with an empirical Brenner II potential and quantum mechanics calculation with PM3. The dynamic formation pathway of the junctions between crossed nanotube pairs was simulated. Junctions were established by forming intertube $sp^3$-related covalent bonds and breaking of bonds in original nanotubes. The final configuration of junctions depends on the chirality of the crossed tube pairs and reaction temperature. Junction formation from nanotubes with larger diameters requires higher temperature.

DOI: 10.1103/PhysRevB.70.125418 PACS number(s): 61.46.+w, 61.72.Cc, 65.80.+n, 81.07.De

## I. INTRODUCTION

Carbon nanotube junctions are promising candidates as building blocks for nanoelectronic devices, because of the remarkable electronic properties of carbon nanotubes. There has been much research exploring the formation and properties of CNT junctions. Intramolecular junctions (IMJs) between carbon nanotubes, such as metal-metal type (MM), metal-semiconductor type (MS) or semiconductor-semiconductor type (SS) junctions, can be created by introducing a single defect or multiple topological pentagon-heptagon (5−7) defects between two different nanotube segments with different atomic and electronic structures.[1–4] An MS junction behaves like a rectifying diode with nonlinear transport characteristics that are strongly asymmetric with respect to bias polarity. In case of MM junction, the conductance appears to be strongly suppressed and displays a power-law dependence on temperature and applied voltage,[5,6] while an SS junction can be designed into light-emitting or laser devices.[7] Multi-terminal heterojunctions, such as crossed CNT junctions,[8–10] "Y," "T," or "X" junctions,[11–17] may also work as transistors. Many attempts have been made to join single-walled nanotubes (SWNTs) to form multiterminal junctions (and ultimately, complex devices). These include welding with electron beam[18–20] or ion beam,[21,22] mechanical manipulation with atomic force microscope,[23,24] nanotube soldering,[18] and chemical functionalization.[25] Terrones *et al.*[19] observed a stable X-shape junction in situ in a transmission electron microscope, and performed tight-binding molecular dynamics calculations to support their observation. Molecular dynamics simulations[20,22] demonstrated that crossed single-walled carbon nanotubes could be joined by electron or ion beam welding to form molecular junctions. They all concluded that no merging of crossed tubes occurred in absence of electron or ion beam irradiation with a tube diameter ranging from 7 to 20 Å, and that exposure to electron or ion beams at elevated temperatures induced structural defects such as vacancies and interstitials, which promoted the joining of tubes via the cross-linking of dangling bonds. Recently, nanotubes with diameters of only 4 Å have been discovered in experiments,[26,27] and the range of possible chiral indices of these ultra thin carbon nanotubes (UTCNTs) is limited to three candidates, namely the armchair (3, 3), the zigzag (5, 0) and the chiral (4, 2). Also, tight-binding molecular dynamics (TBMD) simulations[28] have shown that isolated UTCNTs were thermally stable up to about 3000 K, independent of the chirality. Kawai *et al.*[29–31] performed a TBMD simulation and found that two UTCNTs with or without the same chirality can coalesce to form a new tube with a larger diameter via a zipper-like mechanism without pre-existing structural defects, and UTCNTs with reactive dangling bonds and highly strained bonds display higher chemical reactivity.[28–31]

In the present work, we investigated a simple welding process between UTCNTs using classical molecular dynamics method with an empirical Brenner II interatomic potential.[32] The electronic structures and total energy of junctions were calculated using semi-empirical quantum mechanics method PM3,[33] implemented with HyperChem 7. The main focus of our studies was to investigate the formation mechanism, atomic structures and thermal stability of the junctions formed by joining UTCNT pairs with different chiralities at different temperatures. It was found that UTCNTs with or without the same chirality could bond covalently to form multi-terminal junctions at elevated temperatures without pre-existing structural defects, and that the reaction temperature and chirality of two crossed UTCNTs influenced the final configurations of multi-terminal junctions.

## II. METHOD

Our MD simulations started with two defect-free UTCNTs crossed at an angle of 90°, at an initial wall to wall distance of about 4.0 Å, which is larger than the van der Waals distance of 3.4 Å. Three types of junctions were formed by three pairs of crossed tubes with following chiral indices: $(3,3)-(3,3)$, $(5,0)-(5,0)$, and $(3,3)-(5,0)$. Each pair consisted of 480, 400, and 440 atoms in the simulation cells, respectively. For comparison, we also considered CNTs

 

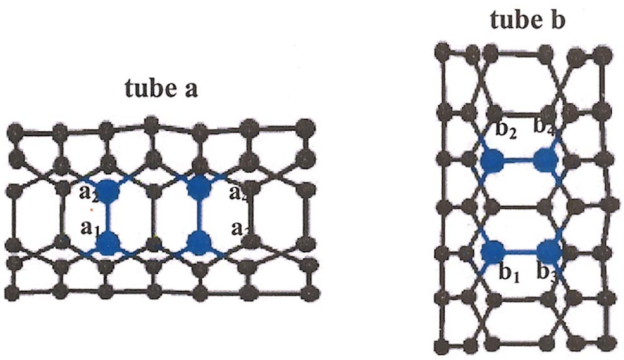


FIG. 1. (Color) Initial configuration of two crossed (3,3) UTCNTs, with atoms ($a_1$-$a_4$ and $b_1$-$b_3$) highlighted in blue which are included in bonding arrangement.

with larger diameters, such as (4, 4) and (6, 0). Periodic boundary conditions were imposed along both nanotube axes, and the lengths of the supercell in the two axis directions were adjusted to match the lattice constant of each nanotube. Molecular dynamic (MD) simulations were done at the following temperatures: 1300, 1500, 1800, 2300, 2500, and 2800 K. The Langevin friction force scheme[34] was applied for temperature control. Time step was kept fixed at 0.5 fs and the total simulation time was 3 ns. Clusters with the junction extracted from MD simulations were optimized using the Polak-Ribiere algorithm until a root-mean-square (rms) gradient less than 0.01 $\mathrm{kcal}\cdot\mathrm{\AA}^{-1}\cdot\mathrm{mol}^{-1}$ was attained. Calculations for total energy and electronic structure of these optimized clusters were performed with PM3 at the restricted Hartree-Fock (RHF) level, and the convergence criterion was that the difference in total energy after two consecutive iterations was less than $10^{-3}$ kcal/mol.

## III. RESULTS AND DISCUSSIONS

In this section we present results obtained from MD and semi-empirical PM3 simulation, and investigate the formation mechanism of multi-terminal junction in crossed UTCNTs, and the effects of reaction temperature and chirality of tubes on the final configuration of junctions. Moreover, we point out that the formation of junctions in CNTs with larger diameters requires higher temperature.

### A. Formation mechanism of multi-terminal junctions in UTCNTs

Two crossed (3, 3) nanotubes were chosen to illustrate the formation mechanism of junctions. The initial configuration of two (3, 3) tubes are shown separately in Fig. 1 to clarify the positions for bond forming and breaking, and atoms in blue are included in the bonding rearrangement. Figures 2(a)–2(i) are snapshots of the welding process at 1800 K, and atoms $a_1$-$b_4$ correspond to those in Fig. 1. The initial configuration was two defect-free $(3,3)-(3,3)$ UTCNTs crossed at an angle of 90° with a wall to wall distance of 4.0 Å. The two nanotubes initially approached each other due to the thermal vibration; and one new $sp^3$-related bond $a_1b_1$ with length of 1.434 Å [denoted in red in Fig. 2(a)] formed after 0.53 ns between the two nanotubes. After 0.565 ns, another $sp^3$-related bond $a_2b_2$ was created, resulting in four $sp^3$-bonded atoms which were denoted in red in Fig. 2(b). At this moment, the $sp^3$-related intratube bond $a_1a_2$ perpendicular to the tube axis [indicated by green arrow in Fig. 2(b)] was stressed greatly due to the large curvature and highly saturated covalent bonds. Therefore, the bond was broken quickly in order to reduce total energy, with two $sp^3$-bonded atoms ($a_1$ and $a_2$) changed into two $sp^2$-bonded atoms shown in blue in Fig. 2(c). After 0.728 ns the third $sp^3$-related intertube bond $a_3b_3$ was formed, together with a highly stressed intratube bond $b_1b_3$ marked by green arrow in Fig. 2(d) (top view, to show the third intertube bond in red distinctly). In the same way, stress was partially released by breaking of this intratube bond [see Fig. 2(e)] after 0.76 ns. At 0.9 ns, the fourth intertube bond $a_4b_4$ was formed, resulting in the generation of two $sp^3$-related intratube bonds ($b_2b_4$ and $a_3a_4$) marked by green arrows in Fig. 2(f). These two $sp^3$-related intratube bonds were still strained and covalently saturate, and were broken successively [shown inFigs. 2(g) and 2(h)] to reduce the total energy further. The entire bonding rearrangement process can be verified by our calculation of electronic structure with PM3 method. Finally, four intertube covalent bonds ($a_1b_1$,$a_2b_2$,$a_3b_3$, and $a_4b_4$) connect the two crossed. (3, 3) UTCNTs and form the sides of four enneagons [Fig. 2(h)]. This covalent junction is symmetric, i.e., all the connections between the four arms of the crossed (3, 3) CNTs are similar in the form of enneagon. Figure 2(i) shows one enneagon (in red circle) in one connected region. Such a bond rearrangement process has been found during the coalescence of two ultra-thin nanotubes.[30] The total number of surplus bonds in the final structure is 12, agreeing with Euler's rule[35] that determines the carbon ring structures in arbitrary $sp^2$-bonded junction structures. An X-shaped multiterminal junction connecting the two perpendicularly crossed nanotubes was clearly established by the topological defects in the form of four enneagons. It was further found that this kind of junction was stable during our simulation time in the temperature range between 1500 and 2300 K. The lower the reaction temperature, the more time is needed to reach the final bonding configuration between the two crossed UTCNTs, for kinetic energy is required to overcome the energy bafflers to form and break bonds. For example, the junction was completely formed after 1.25 ns at 1800 K and after 0.8 ns at 2500 K.

The variation of total energy for all configurations (denoted by squares) during the welding process with respect to the total energy of initial crossed tubes was plotted in Fig. 3. "Initial" is the initial configuration of two crossed (3,3) tubes; "a-h" accords to the configuration in Figs. 2(a)–2(h). The results indicate definitely that the stress can be partially released by forming a junction. The structures (a-h) are fully relaxed, and total energy is calculated using PM3 method. As seen in the figure, an increase in energy (indicating a barrier to the welding process in configuration a-d) is followed by a drop in energy (in configuration e-h); junction formation is energetically favored compared with structures of crossed tubes. Once the barrier is overcome, formation of junction can be driven by the lowering of energy.

The formation mechanism of multi-terminal junction in $(5,0)-(5,0)$ and $(3,3)-(5,0)$ is similar to that in $(3,3)$

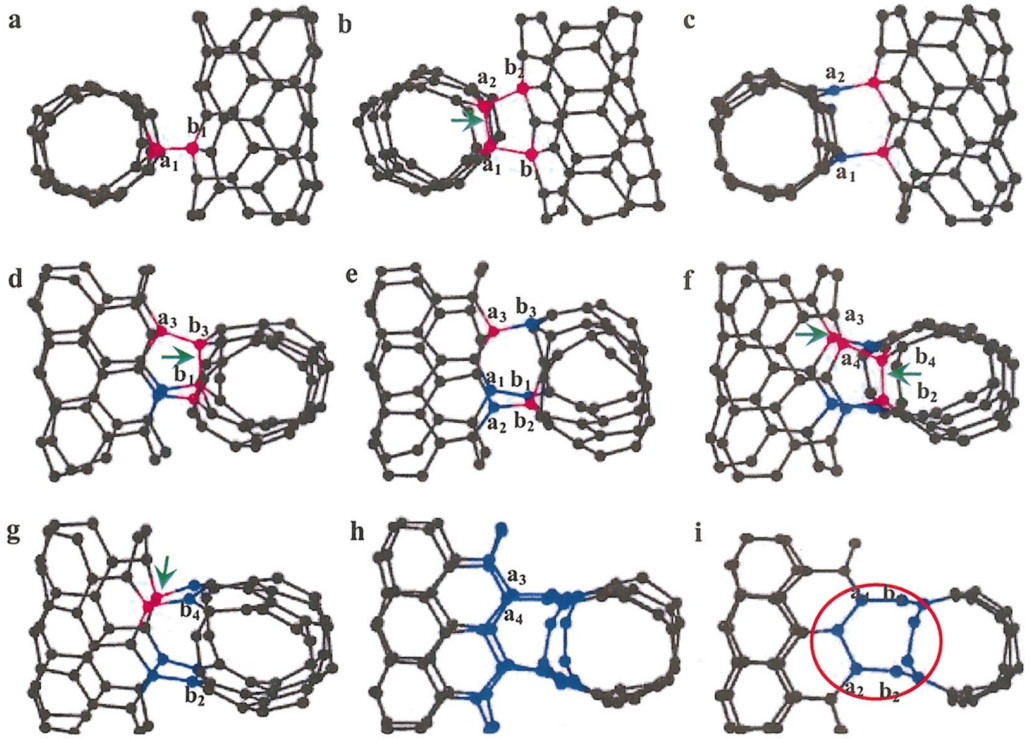


FIG. 2. (Color) Snapshots from simulation of welding two crossed (3,3) UTCNTs at 1800 K (side and top view). (a) After 0.53 ns, two tubes approach each other and one new $sp^3$-related intertube bond $a_1b_1$ with length of 1.434 Å (in red) is formed (side view). (b) After 0.565 ns, another intertube bond $a_2b_2$ (in red) is formed; resulting in a highly stressed and saturated intratube bond $a_1a_2$ denoted by green arrow (side view), which is. broken quickly (c) to release the stress (side view). (d) After 0.728 ns, the third intertube bond $a_3b_3$ is generated (top view), and the strained $sp^3$-related intratube bond $b_1b_3$ marked by green arrow in (c) is broken to reduce the total energy (e). (f) After 0.9 ns, the fourth intertube bond is created, causing two $sp^3$-related intratube bonds ($b_2b_4$ and $a_3a_4$) marked by arrow, which are broken successively in (g) and (h). Connection between two tubes is established through four enneagons (in blue) and one enneagon is shown in (i). $Sp^3$ atoms are highlighted, in red, and $sp^2$ atom in topological defect in blue.

−(3,3). It was suggested that the multi-terminal junctions between two crossing UTCNTs could be created through successive bond rearrangements, i.e., formation of $sp^3$-related intertube bonds and breaking of $sp^3$-related intratube bonds.

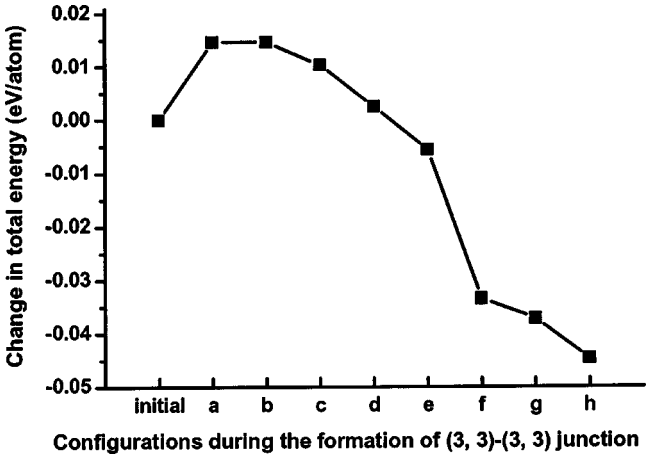


FIG. 3. The variation of total energy for all the configurations (denoted by squares) during the welding process. Initial: the initial configuration of crossed (3,3) tubes with wall to wall distance of 4.0 Å; a-h: configurations corresponding to those in Figs. 2(a)–2(h).

### B. Effects of temperature and chirality on final configuration of multi-terminal junctions

Figures 4 shows the final configurations of junctions formed by joining (3,3)−(3,3),(5,0)−(5,0), and (3,3) −(5,0) pairs at temperatures 1300 K (a), 1800 K (b), 2300 K (c), 2500 K (d), and 2800 K (e) with the simulation time of 3 ns. In all cases, the final configurations of the joints are energetically favorable compared with initial structures of two crossed UTCNTs through single point energy calculations using PM3 method. From these figures, it was concluded that the chirality of the nanotubes and reaction temperature influence the bond rearrangement process, final structure, and bonding properties of carbon atoms around the region of junction.

As the temperature increases, more intertube bonds formed to connect the two crossed tubes and more original bonds are broken during the process of welding, resulting in an expanded junction region, a decrease in the intertube distance, and a high degree of bonding disorder. For both crossed (5,0)−(5,0) and (3,3)−(5,0) UTCNTs, it is obvious that the junction regions at 2500 K [Fig. 4(d)] and 2800 K [Fig. 4(e)] are larger than those at 1300 K [Fig. 4(a)] and 1800 K [Fig. 4(b)], and that there was a notable decrease in the intertube distance at high temperatures [Figs. 4(d) and 4(e)], which may have influence on mechanical properties,[20]

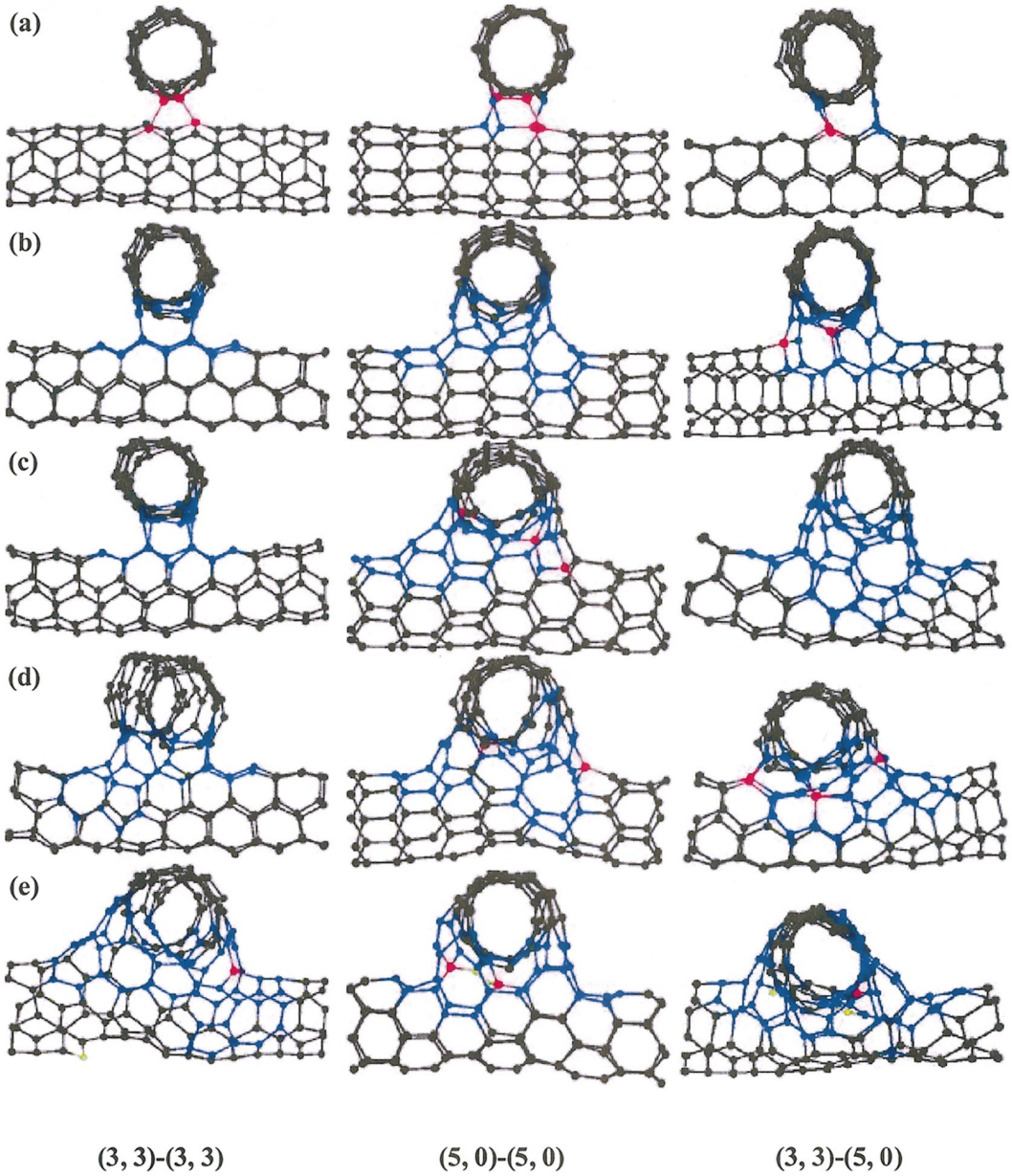


FIG. 4. (Color) Figures 4(a)–4(d) show the final configurations of the multi-terminal junctions between two crossed (3,3)-(3,3), (5,0)-(5,0), and (3,3)-(5,0) UTCNTs at 1300 K (a), 1800 K (b), 2300 K (c), 2500 K (d), and 2800 K (e), with $sp^3$ atoms in red, $sp^1$ atoms in yellow, and $sp^2$ atoms in topological defects in blue. Left column for (3,3)-(3,3) tubes, middle column for (5,0)-(5,0) tubes, and right column for (3,3)-(5,0) tubes.

the I-V properties and Ohmic behavior of the junctions.[17] Although the junctions between two (3, 3) tubes, composed of four enneagons, are smoother and closer to perfection than those between other two types, there is also an extension in the joining region at 2500 K (Fig. 4(d), composed of one pentagon, three heptagons, two octagons and two enneagons) and 2800 K [Fig. 4(e)]. The extended junctions made of only topological defects obtained at higher temperature are more stable. For (3,3)−(3,3) tubes, the formation energy of junction at 1800 K is −0.045 eV/atom, while formation energy of that at 2500 K is −0.142 eV/atom; for (5,0)-(5,0) tubes, the formation energy of junction at 1300 K is −0.02 eV/atom, while that at 1800 K is −0.073 eV/atom. At the same time, tube bending, relative rotation and side movement of two tubes [Figs. 4(c)–4(e)] occur, contributing to the extension of those junctions. Junctions at higher temperature include many miscoordinated ($sp^1$ or $sp^3$) atoms, as well as topological defects. At 2800 K, $sp^1$-bonded atoms highlighted in yellow in Fig. 4(e), present in (3,3)−(3,3),(5,0) −(5,0), and (3,3)−(5,0) junctions. The numbers of bonds formed and broken during the MD simulation of 3 ns are summarized in Table I. Because the conditions are complicated at high temperatures, we just give the numbers during bonding rearrangements at lower temperatures for comparison. The more bond formed and broken, the more topological defects were produced, resulting in extension in junction region. As the temperature increases, the time needed for links to form and bonds to break was reduced; the junctions

TABLE I. Number of bonds formed ($N_f$) and broken ($N_b$) in junctions formed between crossed UTCNTs with different chirality and at different reaction temperature.

| | 1300 K | | 1500 K | | 1800 K | |
|---|---|---|---|---|---|---|
| | $N_f$ | $N_b$ | $N_f$ | $N_b$ | $N_f$ | $N_b$ |
| (3,3)−(3,3) | 2 | 0 | 4 | 4 | 4 | 4 |
| (5,0)−(5,0) | 4 | 2 | 5 | 3 | 8 | 7 |
| (3,3)−(5,0) | 4 | 3 | 9 | 7 | 12 | 10 |

came to contain an increasing number of topological defects, including dangling bonds or $sp^3$-bonded atoms. However, junctions obtained by heating in our study are more ideal than those obtained by ion-beam in Ref. 22 or electron-beam irradiation in Refs. 17 and 20.

The chirality of the pairs of tubes has important effects on the final configuration of junctions, because it influences the welding process. Though all atoms in both junctions formed at 1800 K maintain their $sp^2$ hybridization, the (3,3) −(3,3) junction contains four enneagons, and the (5,0) −(5,0) contains two enneagons, two octagons and two heptagons [Fig. 4(b)]. However, the (3,3)−(5,0) junction at 1800 K still has $sp^3$ atoms, as well as topological defects, as indicated in red in Fig. 4(b). At 2300 K, both (3,3)−(3,3) and (3,3)−(5,0) junctions are made of $sp^2$ atoms, but the former is composed of four enneagons, and the latter composed of three pentagons, four heptagons, four octagons and one enneagon. However, $sp^3$ atoms are included in (5,0) −(5,0) junctions at 2300 K. It was found that topological defects around the (3,3)−(3,3) junction region keep the form of four enneagons from 1500 to 2300 K, representing a more stable and smoother junction than those of (3,3) −(5,0) and (5,0)−(5,0). The sites and numbers of formed and broken bonds are quite different among these different tube pairs. From Table I, one can see that more bonds formed and broken to release the stress in (5,0)−(5,0) and (3,3) −(5,0) pairs than those in (3,3)−(3,3) pairs at the same temperatures, since strain energy in zigzag tube is larger than that of armchair tube over all range of diameters.[36]

Since the bond forming and breaking determines the final configurations of junctions, all the factors influencing the bond rearrangement can affect the formation process of junctions. For nanotubes under compression (reducing the wall to wall distance) and molecular atmosphere (such as $O_2$,$N_2$) or under conditions with transition metal atoms (such as Ti,[37] Fe), junctions with different final structures and properties may be generated, which need further study.

### C. Multi-terminal junctions in CNTs with larger diameters

It was found from our simulation that the nanotubes with a. little larger diameters, the temperature required for junction formation is higher: A stable junction in (4,4)−(4,4) tube pairs, including only topological defects, can be created at 3200 K, and (5,5)−(5,5) junction made of $sp^2$ atoms can be generated at temperature higher than 3500 K. The junction in (6,0)−(6,0) tube pairs, composed of topological defects in form of two heptagons, two octagons, and two enneagons, can be created at 2500 K, while this kind of junction in (5,0)−(5,0) tube at 1800 K. The curvature plays an important role in the formation of junctions. For CNTs with even larger diameters, such as (10,10)−(10,10) and (12,0)−(12,0) tubes, no junctions were found in our simulation with total simulation time of 3 ns even at 4000 K where topological defects can form on the wall of tubes, consistent with the conclusion in Refs. 19–22 that no merging of crossed tubes occurred in the absence of electron or ion beam irradiation. Therefore, it is suggested that nanotubes with a little larger diameters can be welded to form multiterminal junctions only at higher temperatures, without initially introduced defects.

## IV. CONCLUSION

It was shown by our MD simulation that multiterminal junctions of UTCNTs can be formed by heating two crossed UTCNTs without pre-existing structural defects. The link between the two crossed tubes is established through formation of intertube $sp^3$-related covalent bonds and breaking of original intratube bonds, which results in junctions composed of topological defects. The high stress can be partially released by the formation of junctions. The welding processes and final configurations of junctions depend on the chirality of the crossed nanotube pair and temperature. A higher temperature will result in a broader junction region, a reduced intertube distance and large degree of bonding disorder, due to more bonds formed and broken, rotation and lateral movement of crossed UTCNTs. The time needed for a complete welding of the two crossed UTCNTs decreases as the temperature increases. $Sp^1$ hybrided atoms may present at elevated temperatures. Higher temperature is required for CNTs with a little larger diameters to generate multi-terminal junctions.

## ACKNOWLEDGMENTS

This work was partially supported by research grants from Hong Kong Polytechnic University (A-PE54) and the Research Grants Council of Hong Kong (B-Q747). Xu and Yang acknowledge the support from the Ministry of Science and Technology of China under Grant No. TG2000067105.

*Corresponding author. Electronic address:
mmsqshi@polyu.edu.hk

[1] B. I. Dunlap, Phys. Rev. B **46**, 1933 (1992); **49**, 5643 (1994).
[2] J. Han, M. P. Anantram, R. L. Jaffe, J. Kong, and H. Dai, Phys. Rev. B **57**, 14983 (1998).
[3] L. Chico, V. H. Crespi, L. X. Benedict, S. G. Louie, and M. L. Cohen, Phys. Rev. Lett. **76**, 971 (1996).
[4] L. Chico, L. X. Benedict, S. G. Louie, and M. L. Cohen, Phys. Rev. B **54**, 2600 (1996).
[5] Z. Yao, H. W. Ch. Postma, L. Balents, and C. Dekker, Nature (London) **402**, 273 (1999).
[6] M. Ouyang, J. L. Huang, C. L. Cheung, and C. M. Lieber, Science **291**, 97 (2001).
[7] H. J. Kim, J. Lee, S. J. Kahng, Y. W. Son, S. B. Lee, C. K. Lee, J. Ihm, and Y. Kuk, Phys. Rev. Lett. **90**, 216107 (2003).
[8] M. S. Fubrer, J. Nygård, L. Shih, M. Forero, Y. G. Yoon, M. S. C. Mazzoni, H. J. Choi, J. Ihm, S. G. Louie, A. Zettl, and P. L. McEuen, Science **288**, 494 (2000).
[9] Y. G. Yoon, M. S. C. Mazzoni, H. J. Choi, J. Ihm, and S. G. Louie, Phys. Rev. Lett. **86**, 688 (2001).
[10] A. Nojeh, G. W. Lakatos, S. Peng, K. Cho, and R. F. W. Pease, Nano Lett. **3**, 1187 (2003).
[11] M. Menon and D. Srivastava, Phys. Rev. Lett. **79**, 4453 (1997).
[12] M. Menon and D. Srivastava, J. Mater. Res. **13**, 2357 (1998).
[13] M. Menon, D. Srivastava, and S. Saini, Semicond. Sci. Technol. **13**, A51 (1998).
[14] A. P. Garrido and A. Urbina, Carbon **40**, 1227 (2002).
[15] M. Menon, A. N. Andriotis, and D. Srivastava, Phys. Rev. Lett. **91**, 145501 (2003).
[16] I. Ponomareva, L. A. Chemozatonskii, A. N. Andriotis, and M. Menon, New J. Phys. **5**, 119 (2003).
[17] F. Cleri, P. Keblineski, I. Jang, and S. B. Sinnott, Phys. Rev. B **69**, 121412(R) (2004).
[18] F. Banhart, Nano Lett. **1**, 329 (2001).
[19] M. Terrones, F. Banhart, N. Grobert, J. C. Charlier, H. Terrones, and P. M. Ajaya, Phys. Rev. Lett. **89**, 075505 (2002).
[20] I. Jang, S. B. Sinnott, P. Danailov, and P. Keblinski, Nano Lett. **4**, 109 (2004).
[21] B. Ni, R. Andrews, D. Jacques, D. Qian, M. B. J. Wijesundara, Y. Choi, L. Hanley, and S. B. Sinnort, J. Phys. Chem. B **105**, 12719 (2001).
[22] A. V. Krasheninnikov, K. Nordlund, J. Keinonen, and F. Banhart, Phys. Rev. B **66**, 245403 (2002).
[23] J. Lefebvre, J. F. Lynch, M. Llaguno, M. Radosavljevic, and A. T. Johnson, Appl. Phys. Lett. **75**, 3014 (1999).
[24] H. W. Ch. Postma, M. de Jonge, Z. Yao, and C. Dekker, Phys. Rev. B **62**, R10653 (2000).
[25] P. W. Chiu, G. S. Duesberg, U. D. Weglikowska, and S. Roth, Appl. Phys. Lett. **80**, 3811 (2002).
[26] L. C. Qin, X. L. Zhao, K. Hirahara, Y. Miyamoto, Y. Ando, and S. Iijima, Nature (London) **408**, 50 (2000).
[27] N. Wang, Z. K. Tang, G. D. Li, and J. S. Chen, Nature (London) **408**, 50 (2000).
[28] T. Kawai, Y. Miyamoto, O. Sugino, and Y. Koga, Phys. Lett. B **323**, 190 (2002).
[29] M. Kostov, H. Cheng, A. C. Cooper, and G. P. Pez, Phys. Rev. Lett. **89**, 146105 (2002).
[30] T. Kawai, Y. Miyamoto, O. Sugino, and Y. Koga, Phys. Rev. Lett. **89**, 085901 (2002).
[31] M. Terrones, H. Terrones, F. Banhart, J. C. Charlier, and P. M. Ajayan, Science **288**, 1226 (2000).
[32] D. W. Brenner, Phys. Rev. B **42**, 9458 (1990); D. W. Brenner, O. A. Shenderova, J. A. Harrison, S. J. Stuart, B. Ni, and S. B. Sinnott, J. Phys.: Condens. Matter **14**, 783 (2002).
[33] J. J. P. Stewart, J. Comput. Chem. **10**, 209 (1989).
[34] J. C. Tully, Y. J. Chabal, K. Raghavachari, J. M. Bowman, and R. R. Lucchese, Phys. Rev. B **31**, 1184 (1985).
[35] V. H. Crespi, Phys. Rev. B **58**, 12671 (1998).
[36] D. H. Oh and Y. H. Lee, Phys. Rev. B **58**, 7407 (1998).
[37] N. Gothard, C. Daraio, J. Gaillard, R. Zidan, S. Jin, and A. M. Rao, Nano Lett. **4**, 213 (2004).